IDENTIFICATION OF *WHITE NOISE* AND *1/f* IN CURRENT MIRROR CONFIGURATION BASED ON V_{DS} MOSFET

Maria Rosariana Gea[1], Lazuardi Umar[*1], Rahmondia Nanda Setiadi[1]
[1]*Department of Physics, University of Riau, Jl. Prof. Muchtar Luthfi Pekanbaru, 28293, Indonesia*
[*]*e-mail*: lazuardi@unri.ac.id

ABSTRACT

Identifying noise in the Current Mirror (CM) circuit is essential to locate noise signals in biosensor applications so that measurements become more accurate and precise. There are two dominant types of noise: white noise, which consists of thermal noise and shot noise, and also low-frequency noise (1/f noise). The main component of the CM circuit is the BS250 type MOSFET, which works by varying the width of the charge carrier channel controlled by the voltage at the gate. When the drain is given a voltage, electrons will flow from the source to the drain which generates the noise. This study was carried out to identify the noise in the CM configuration by varying the reference voltage of MOSFET using the PCI-6221 card data integrated with the LabVIEW program. The reference voltage values used are 1 mV, 10 mV, and 100 mV to determine the effect of the input voltage on the CM circuit noise signal, while the measurement frequency is varied from 0.1 Hz to 100 kHz with a resolution of 0.1 Hz. The results show that the noise characteristics vary with the applied voltage, which will increase at a higher voltage. Analysis of 1/f noise at frequencies up to 0.2 Hz has a gradient increase of up to 10 times for each given voltage value. Based on the value of the data distribution on the white noise measurement, it shows that a voltage of 100 mV produces the highest noise with an average of $3.62 \times 10\text{-}7$ $V_{rms}/Hz^{1/2}$. The results of this study are used in the design of CM circuits with minimal noise.

Keywords : Biosensor; Current Mirror; MOSFET BS250; White and *1/f* Noise

INTRODUCTION

The biosensor application has an interface between the biological object and the transducer substrate using a sensitive surface layer when interacting with the analyte solution (Ziegler, 1998). A biosensor system using a current mirror circuit has been designed and characterized. The Current Mirror (CM) circuit changes the input current without loading to minimize the current loss at the output (Wang, 2017), which generally consists of two Metal Oxide Semiconductor Field Effect Transistors (MOSFETs). One of the transistors will duplicate the input current of the MOSFET mainline current that works in biosensor measurements (Umar, 2019).

The active component of the MOSFET is the largest source of noise in the CM circuit due to the random movement of electrons in the conductor, the presence of potential barriers, and noise that occurs due to low frequencies (Vasilescu, 2005). Wati (2020) has characterized the noise at the input and output of a MOSFET-based CM circuit by varying the value of the resistor used in the circuit. Noise is a spontaneous fluctuation of voltage or current generated by electronic system components and depends on the fabrication process and environmental conditions (Wilamowski, 2018). The high noise causes high voltage consumption by the tool. The increasing demand for portable devices with low consumption requires a combination of components that can work optimally (Singh, 2018).

The study aims to determine the reference voltage effect on the noise signal generated by the CM circuit. Noise is analyzed using the PCI-6221 card integrated with the LabVIEWprogram, graph of noise against frequency is obtained. The frequency range used is by the performance of a vast biosensor system, namely 0.1 Hz to 100 kHz. The voltages used for the CM circuit are 1 mV, 10 mV, and 100 mV, so that the current will increase in the circuit, while for the measurement a 10 kΩ resistor is used for reference (R_{ref} and R_L) to prevent the temperature change due to resistance in the circuit.

METHOD

MOSFET Electronic Components

MOSFET components work in three operational areas, namely saturation, cut-off, and linear. No current will flow when the gate voltage is less than the threshold voltage and the MOSFET is in the cut-off region. When the drain is given a small voltage, the current will flow from drain to the source so that a channel with resistance and MOSFET is formed in the linear region. The drain

current (I_D) is proportional to the value of the drain to source voltage, shown by equation (1):

$$I_D(LIN) = k_n \left(V_{GS} \quad V_T\right)V_{DS} \quad \frac{V_{DS}^2}{2} \tag{1}$$

The saturation area of the transistor will occur if the applied voltage increases continuously so that the gate becomes neutral, hence the inversion layer on the drain side will disappear. The V_{DS} voltage results in a larger reverse bias from online to the body than from source to the body. Transconductance is a measure of current sensitivity to changes in gate-source bias (Barkhordarian,1996). This parameter is influenced by the maximum gate width, which is proportional to V_{DS}. A parameter that determines the work of a MOS is threshold voltage. This parameter is important in MOSFET modeling and is extracted from the current or capacitance characteristics measured using one or more transistors (Ortiz, 2002). The physical form of the BS250 MOSFET used in this study is shown in Figure 1.

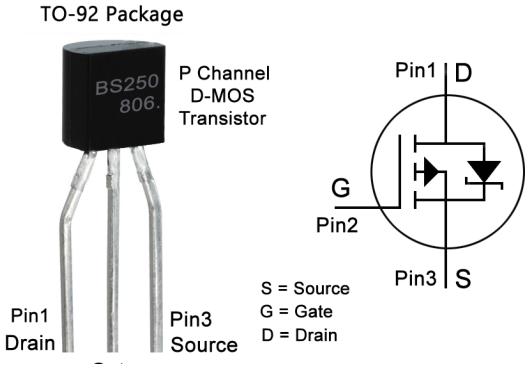

Figure 1. MOSFET electronic components

Noise in *Current Mirror*

The biosensor application applies a CM circuit to convert the current through the sensor into a voltage with the principle of duplication where the same input and output current will evaluate the signal from the biosensor. CM circuits with efficient designs are widely used as the basic unit in current amplification, biasing, and dynamic loads in various analog circuits (Aggarwal, 2016). The CM module uses fewer components, resulting in low power consumption. The FET transistor is the main component of the circuit to duplicate the current from one element by controlling the current in other active parts so that the output current remains constant. The load resistance (R_L) and input (R_{ref}) have the same value so that no gain occurs. Noise of CM circuit is analysed using the equivalent circuit, depicted in Figure 2:

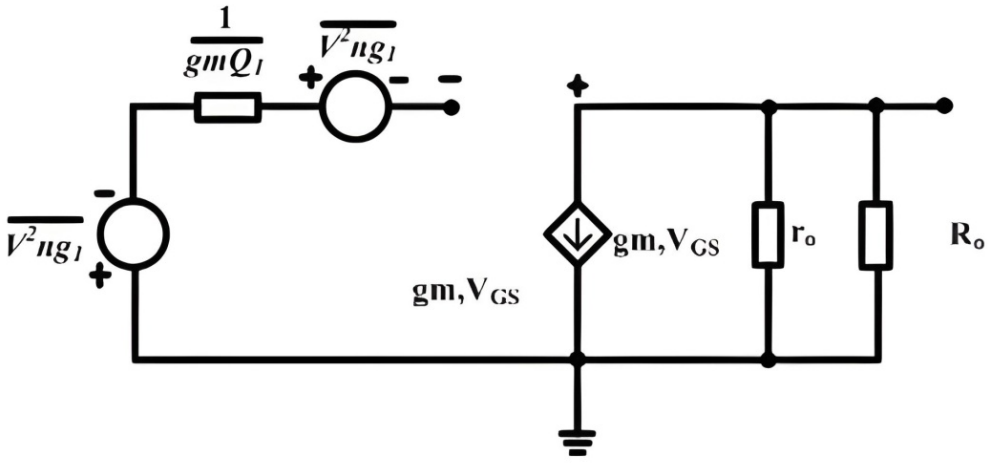

Figure 2. CM equivalent circuit (Wati, 2021)

Noise in the CM circuit is divided into two types: white noise e_{ow} due to shot noise and frequency e_{of} causing thermal noise (Kiely, 2017). Shot noise comes from the current flowing in the circuit, which will increase when source line voltage is very low (VDS<5kT/q).

$$\frac{V_{sh}^2}{f} = \frac{I^2}{gm^2} = \frac{2q}{I_D}\left(\frac{nkT}{q}\right)^2 \qquad (2)$$

White noise is dominated by thermal noise when the drain current becomes very small. The MOSFET produces a thermal noise of:

$$i_d^2 = 4kT\left(\frac{2}{3}gm\right) f = 4kT\frac{2}{3}\left(gm1 + A^2 gm2\right) f \qquad (3)$$

Fluctuations in the number of electron charges cause $1/f$ noise in n-MOS, and fluctuations in electron mobility charge cause $1/f$ noise in p-MOS (Silvaco, 2009). *Noise 1/f* occurs at low frequencies (<1 Hz). The cut-off frequency acts as a link between white noise and low-frequency noise.

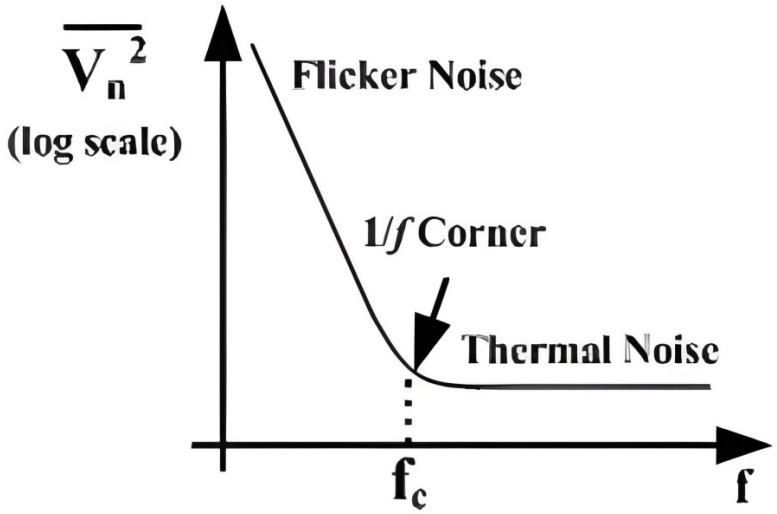

Figure 3. Frequency *cut-off*

The CMOS fabrication process expressed in the empirical model generates the *1/f noise* distribution so that noise fluctuations occur in current and voltage. This model can be defined by the following equation:

$$V_n^2 = \frac{K_F}{Cox^2\, WL}\frac{1}{f} \qquad (4)$$

The CM configuration uses the drain and gate channels of Q_1 to be connected, that the transistor operates in saturation mode if $I_{D1}\neq 0$ applies the equation (Umar, 2019):

$$I_{D1} = \frac{1}{2}k_{n1}^{'}\frac{W_1}{L_1}(V_{GS} - V_{t1})^2 \qquad (5)$$

MOSFET components used in CM circuits have different structures and constituent materials. This results in a difference in the flow of electrons in it, resulting in leakage current. In the operation of the microchip, there is also a temperature change. These factors can cause noise in the CM circuit. The value of R_{ref} is the same as R_L, and it will not give any gain to the output. So the output current of the dual transistor pair on the MOSFET will be the same as that of the single transistor. However, the composition of the dual transistor is different for each transistor.

Measurement Set-Up

The circuit components are two BS250 type MOSFETs with BS170 type MOSFETs as a balancer for the input voltage, a capacitor (47 µF), and two resistors with the same value (R_{ref} and R_L). The specifications of the BS250 MOSFET are shown in Table 1.

Table 1. BS250 MOSFET Specifications

Parameter	Symbol	Limitation	Unit
Drain-Source Voltage	$-V_{DSS}$	60	V
Drain-Gate Voltage	$-V_{DGS}$	60	V
Gate-Source-Voltage (pulsed)	V_{GS}	±20	V
Storage Temperature Range	T_S	-60 ke +150	°C

The reference voltage does not experience interference when forwarded to the output, and the Op-amp is used as a buffer. A PCI-6221 card acquires the output signal from the circuit with a 16-bit resolution, which controls the input voltage in the measurement process. This card is integrated with LabVIEW 2020 software as a data processor with a sampling speed of 250 Kbps. Noise data is processed with the Fast Fourier Transform (FFT) function so that it can be displayed in graphic form with 1000+ algorithms.

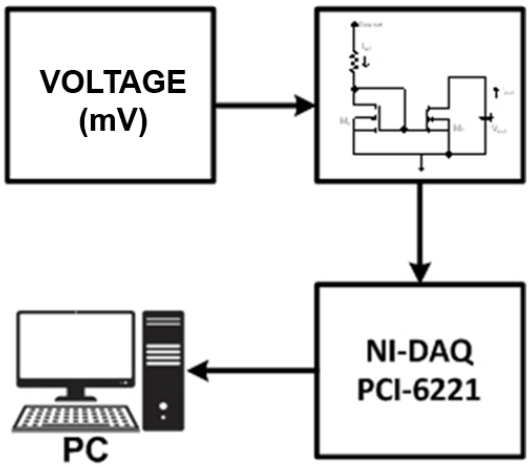

Figure 4. Block diagram of white noise measurement and characterization on Current Mirror

The design of the noise test circuit connected to the PCI-6221 card via the DB37 connector is shown in the following Figure 5. The design of the noise test circuit connected to the PCI-6221 card via the DB37 connector is shown in Figure 2 below. The geometric characteristics of the two MOSFETs are identical, so that the output current ID2 is the same as ID1. The voltage (VDS) causes Q1 to be in the saturation region, while Q2 will be in the saturation region if the saturation voltage is lower than the output voltage (Vout).

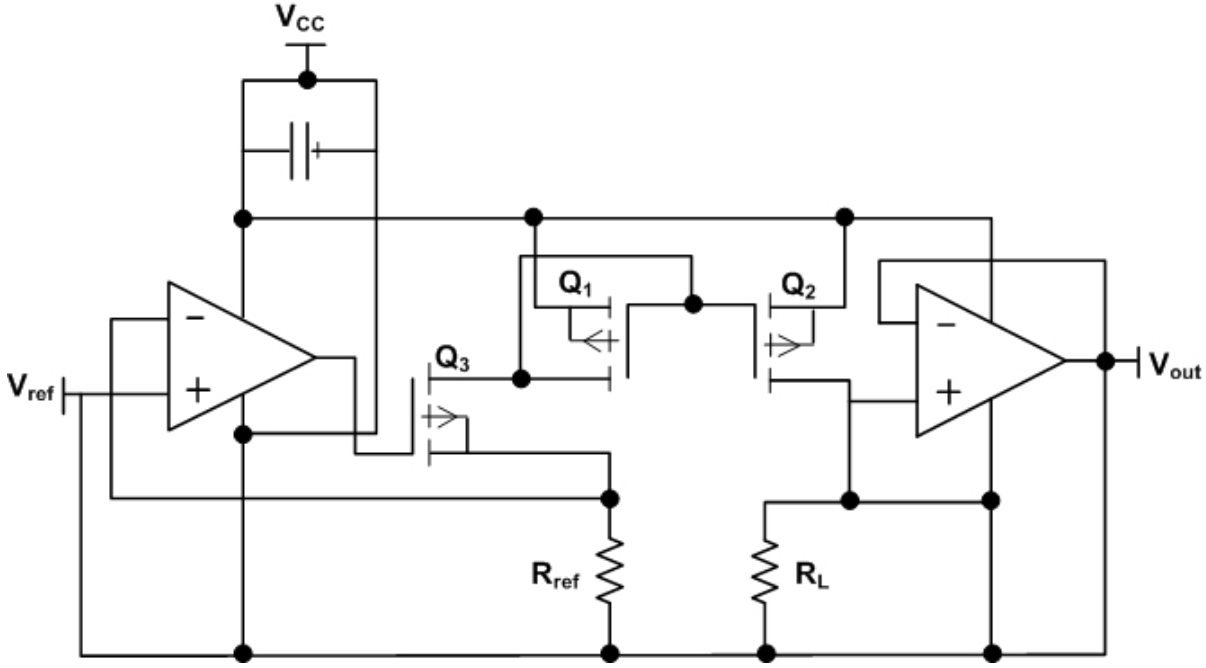

Figure 5. Current Mirror Circuit Platform Design

The MOSFET component is activated by a voltage source (V_{CC}) that comes from a dry battery so that there are no wrinkles that can interfere with noise measurements. The PCI-6221 card has 37 pinouts consisting of analog inputs (16 pins), digital I/O (10 pins), and analog outputs (10 pins). Noise calibration is performed on the PCI-6221 pinout to determine the built-in noise level without any load from the circuit. Voltage variations are fed into the CM circuit with values of 1 mV, 10 mV, and 100 mV. The frequency domain is set from 0.1 Hz to 100 kHz in order to eliminate external noise from PLN grids and cables using a shielding feature. The measurement results from the LabVIEW software will be saved in text format and then analyzed with Igor software, which produces a noise signal graph. Figure 6 shows the shape of the PCI-6221 card.

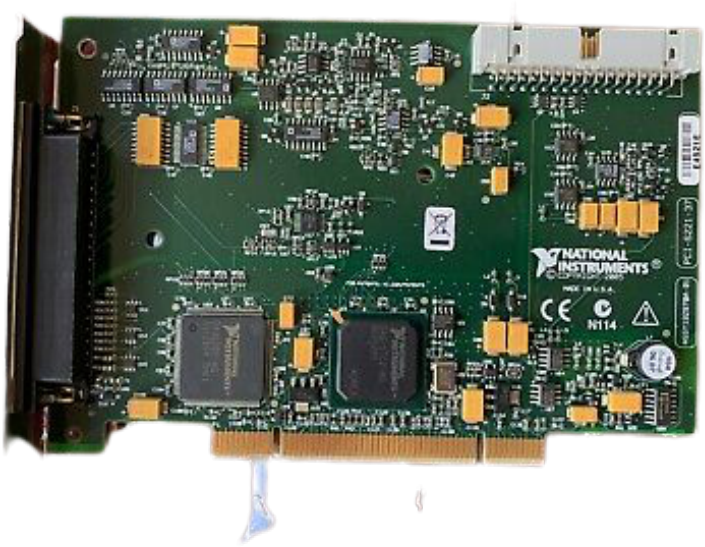

Figure 6. Physical form of NAQ DAQ PCI-6221 card

There are several features, namely 24 digital I/O lines, 16 analog inputs, two analog outputs, and two counters and timers. The PCI slot connects the NI DAQ PCI-6221 card to the computer mainboard. Several other modules are integrated because the DAQ PCI-6221 cannot be used directly as a factory interface.

Table 2. Specifications for NI DAQ PCI-6221 card

Spesifications	Description
Number of channels	8 *differential*or 16 single
ADC Resolution	16 bits
Single-multi-channel data snippet	250 kS/s
Time accuracy	50 ppm/ sampel rate
Time resolution	50 ns
Input Range	±0.2 V, ±1 V, ±5 V, ±10 V
Maximum analog voltage	±11 V
CMRR (DC to 60 Hz)	92 dB

External noise originating from electrical signals in a noise environment is eliminated using a X5 box with dimension of 14.5 cm x 9.5 cm x 5 cm high. The circuit is implemented on a mini solderless breadboard with single terminal strip. The circuit display connected to the PCI-6221 card via the DB37 connector is shown in Figure 6.

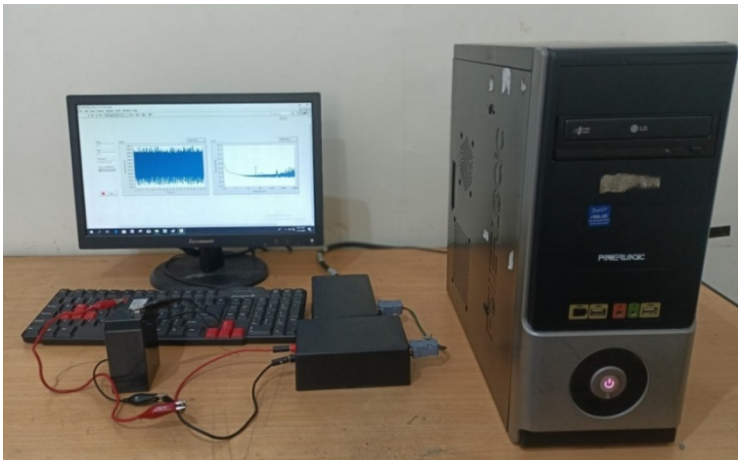

Figure 6. Noise measurement set-up

The frequency domain is set from 0.1 Hz to 100 kHz to remove external noise from the PLN network and cables using the shielding feature. The final data is displayed in the form of the FFT function, and each noise is identified in quantitative and qualitative formats. This study will obtain the characteristics of the circuit, the quality of the measurement signal, and the contribution of noise to each measurement object. The data results are the ratio of noise (Vrms/Hz1/2) to frequency bandwidth. This noise ratio is used as a step to remove noise with the most significant ratio so that the biosensor application is more accurate and has a high level of sensitivity.

RESULTS AND DISCUSSION

The noise measurements with various input voltages are shown in Figure 3, where white noise is analyzed in the frequency range of 1 Hz to 100 kHz. The voltage variation seen in the figure produces different noises, where a higher voltage will produce higher noise. The cut-off frequency that separates 1/f and white noise is 0.2 Hz, where the graph flattens out to 100 kHz. The 1/f noise graph appears linear, with the noise power decreasing to 10-5 $V_{rms}/Hz^{1/2}$ as the frequency increases.

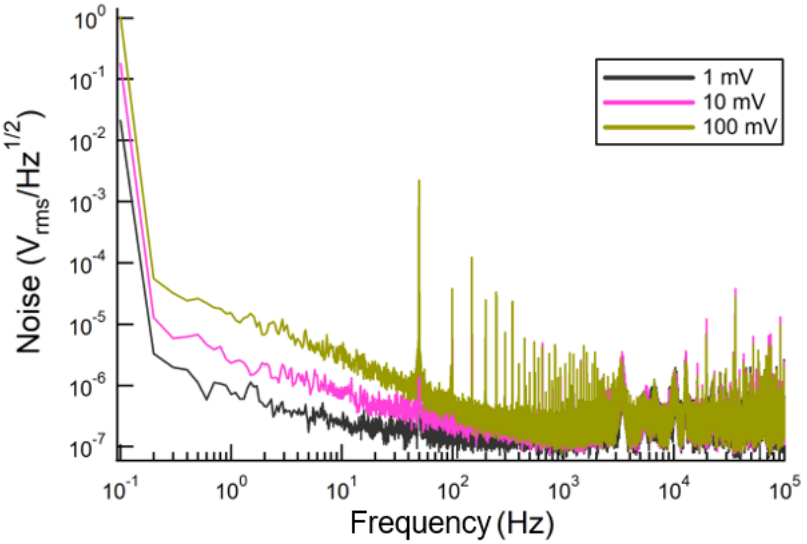

Figure 7. Characterization of white noise with voltage variations (1 mV, 10 mV, 100 mV)

The high bias voltage condition in the drain results in ionization-induced shot noise and produces excess thermal noise in the channel. The noise signal from measurement with input voltage variation did not increase significantly. White noise is analyzed at frequencies ranging from 1 Hz to 100 kHz, where the graph is flat. Based on the measurements, the frequency of 1 Hz to 100 Hz is a noise signal of 10-6 $V_{rms}/Hz^{1/2}$ with a reference voltage of 1 mV and increases in proportion to the

input voltage. This happens because white noise is dominated by thermal noise independent of the applied voltage variable. After all, the extra energy supplied to the free electrons by the field is negligible concerning thermal energy. Signal noise increases at a frequency of 50 Hz due to AC from the power plant.

Statistical parameters of noise measurements with voltage variations are shown in Table 3.

Table 3. Statistical parameter of noise measurement with voltage variation (VDS)

V(mV)	Standar Deviasi, SD ($V_{rms}/Hz^{1/2}$)	Noise ($V_{rms}/Hz^{1/2}$)
1	3.73×10^{-7}	3.29×10^{-7}
10	11.5×10^{-7}	3.59×10^{-7}
100	30.5×10^{-7}	3.62×10^{-7}

The condition of the high bias voltage at the drain causes the ionization-induced shot noise and produces excessive thermal noise in the MOSFET channel. The current fluctuation due to the difference in charge is known as shot noise (Beenakker, 2006). Based on the measurements, the *1/f* noise characterization was analyzed in the frequency range up to 0.2 Hz. The measurement results are shown in Figure 4. 1/f noise measurement uses the same variable voltage as the white noise measurement. the frequency range used is up to 0.2 Hz because this noise occurs in the low frequency range.

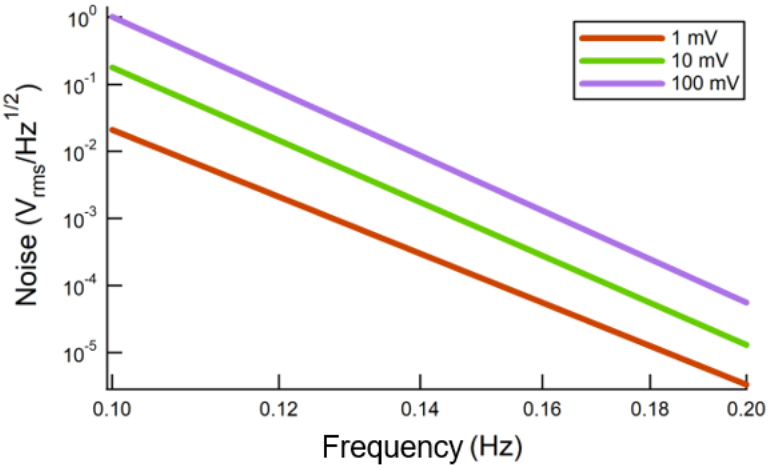

Figure 8. Characterization of white noise with voltage variations

The *1/f noise* curve has a negative gradient, as shown in Figure 4 that the noise decreases at higher frequencies. The slope value of the graph is shown in Table 4.

Table 4. Slope value of 1/f noise graph

V (mV)	1	10	100
Slope ($V_{rms}.Hz^{-3/2}$)	-0.1475	-1.2628	-7.2317

The noise signal with an input voltage of 10 mV to 100 mV has a noise average that is almost the same which can be seen in Table 3 that the average noise does not change significantly. The circuit with an input voltage of 1 mV has a greater slope because it is in the low noise range. The characterization results show that the flicker noise is affected by the input voltage in the circuit. The 1/f noise level at reverse bias remains dependent on charge carrier saturation and lifetime.

CONCLUSIONS

Measurements of the noise response have been made to the 1 mV, 10 mV, and 100 mV reference voltage variations in the CM circuit. The noise was analyzed from 0.1 Hz to 100 kHz using the PCI-

6221 card data acquisition device. Based on the measurement results obtained, noise increases when the voltage rises. The cut-off frequency as the separator between white noise and *1/f noise* is 0,2 Hz. At this frequency, the noise graph will flatten to 100 kHz. Measurements show *1/f noise* increases in proportion to the applied voltage. Based on the statistical parameters of the white noise measurement, it appears that the noise increases in proportion to the applied voltage.

ACKNOWLEDGMENT

This authors acknowledge the Ministry of Education and Culture of the Republic of Indonesia for the funding through the 2022 DRPM Basic Research Program Fund, contract no. 051/E5/PG.02.00.PT/2022.

REFERENCES

Aggarwal, B., Gupta, M., & Gupta, A. K. (2016). A comparative study of various current mirror configurations: Topologies and characteristics. *Microelectronics Journal*, *53*, 134-155.

Barkhordarian, V. (1996). Power MOSFET basics. *Powerconversion and Intelligent Motion-English Edition*, *22*(6), 2-8.

Beenakker, C. W. J., & Schonenberger, C. (2006). Quantum shot noise. *arXiv preprint cond-mat/0605025*.

Kiely, B.R. (2017). Understanding and Eliminating 1 / f Noise. (May). Hal. 3–6

Silvaco .(2009). Noise Modeling in MOSFET and Bipolar Devices Noise Modeling - MOSFET Noise. *Silvaco*.

Singh, M. & Sarma, R. (2018). Design and implementation of MOSFET Based Folded Cascode Current Mirror. *Proceedings - 2nd International Conference on Intelligent Circuits and Systems, ICICS 2018*, (April). Hal. 22–27.

Vasilescu, G. (2005). *Electronic noise and interfering signals: principles and applications*. Springer Science & Business Media. Hal 1-12.

Wang, Z., Chen, Y., Patil, A., Jayabalan, J. dan Zhang, X. (2017). Current Mirror Array : A Novel Circuit Topology for Combining Physical Unclonable Function and Machine Learning. Hal. 1–13

Wati, A., Setiadi, R. N., & Umar, L. (2021, March). Noise characterization of MOSFET current mirror circuit on high impedance application using DAQ card PCI-6221. In *AIP Conference Proceedings* (Vol. 2320, No. 1, p. 050001). AIP Publishing LLC.

Wilamowski, B. M., & Irwin, J. D. (Eds.). (2018). *Fundamentals of industrial electronics*. CRC Press. Hal 58-62.

Umar, L., Hamzah, Y. dan Setiadi, R.N. (2019). Biosensor signal improvement using current mirror topology for dissolved oxygen measurement. *Measurement Science and Technology*. Vol. 30, no. 6, hal. 1-9. https://doi.org/10.1088/1361-6501/ab0675

Ziegler, C., & Göpel, W. (1998). Biosensor development. Current opinion in chemicalbiology, 2(5),585